



**Research Article**

## **Development of CMIP5 Ensemble-Based Climate Change Scenarios for Western Ghats of India**

BAPPA DAS<sup>1\*</sup>, LALU DAS<sup>2</sup> AND SAURAV SAHA<sup>3</sup>

<sup>1</sup>*ICAR-Central Coastal Agricultural Research Institute, Old Goa-403402, Goa*

<sup>2</sup>*Bidhan Chandra Krishi Viswavidyalaya, Mohanpur-741252, West Bengal*

<sup>3</sup>*ICAR Research Complex for NEH Region, Mizoram Centre, Kolasib, Mizoram*

### **ABSTRACT**

Precise assessments of global climate model (GCM) outputs are important for making decisions regarding agriculture, water resources, and ecosystem management. In the current study, temperature and precipitation projections were developed using multi-model ensemble of GCMs for Western Ghats. The performance of Coupled Model Inter-comparison Project 5 (CMIP5) GCMs was evaluated based on the mean annual cycle, temporal trends and Taylor plotting with respect to observed temperature and precipitation over Western Ghats. The best performing models selected were BNU-ESM, CESM1-WACCM, MIROC-ESM-CHEM, MIROC-ESM, MPI-ESM-LR, MPI-ESM-MR, MPI-ESM-P, NorESM1-M, and NorESM1-ME for temperature, while for rainfall CMCC-CMS, EC-EARTH, GFDL-CM3, GFDL-ESM2G, GFDL-ESM2M, MIROC5, MPI-ESM-MR and NorESM1-M were selected. Then the ensemble of best performing models was developed for both temperature and rainfall. The results revealed that the CMIP5 GCM ensemble mean temperature and precipitation are closer to observed values than any individual GCM.

**Key words:** Western Ghats, global climate models, temperature, precipitation, climate projections

### **Introduction**

Climate change became one of the major global concerns for its widespread impact on food production, ecosystem services, drinking water supply, human health, etc. Predictions of the global mean surface temperature and precipitation prove to be of little use as the climate is highly variable at the hemispheric and continental scale. Therefore, the UN Framework Convention on Climate Change in Rio de Janeiro (1992) stressed on the regional scale assessment of climate change pattern and impacts. Since then, several studies have been conducted in different regions worldwide, e.g. Scandinavia and New Zealand (Kidson and Thompson, 1998),

Norway (Benestad, 2002), India (Chaturvedi *et al.*, 2012; Das *et al.*, 2012), Western Himalayan region (Das *et al.*, 2014), South Asia (Das *et al.*, 2015), Punjab, India (Kaur *et al.*, 2020) and Philippines (Daron *et al.*, 2018) using different General Circulation Models (GCMs). Though GCMs have the greatest potential for developing regional climate change scenarios, their ability to reproduce local climatic conditions is restricted (Grotch and MacCracken, 1991). Because GCMs have a coarse resolution and impact analysts are demanding finer resolution in climate change scenarios, numerous approaches to improve resolution have been developed (Daron *et al.*, 2018; Gharbia *et al.*, 2016). Among the various methodologies, statistical downscaling methods, seeking relationships between the GCM simulated variables offered acceptable

\*Corresponding author,  
Email: bappa.iari.1989@gmail.com

scenarios (Das and Akhter, 2019; Huth and Kyselý, 2000).

India is primarily dependent on agriculture for its economy and a large part of the Indian population is engaged in agricultural activities. In spite of increased production of food crops through the ‘green revolution’, Indian agriculture is still heavily dependent on monsoon rainfall, and thus vulnerable to climate change. As Indian climate is predominantly monsoonal climate, so studies on regional monsoon dynamics became one of the most important branches of atmospheric research in India. Though several studies on the intensity of the Indian monsoon showed significant long-term trends on a smaller scale in various parts of India (Singh *et al.*, 2021), instrumental records of monsoon rainfall over the previous century lacked trends on a national scale (Kripalani *et al.*, 2003). Recent studies showed that rainfall will increase by 4 to 5% in near future (2030s) and 6 to 14% at the end of this century (2080s) with an increase in the mean annual surface air temperature by 1.7–2°C and 3.3–4.8°C for those respective periods relative to the 1961–1990 baseline for India (Chaturvedi *et al.*, 2012). Greenhouse gas warming simulations indicated an increased intensity of Asian summer monsoon (Hirakuchi and Giorgi, 1995) with some exceptions (Lal *et al.*, 1994). Based on various GCM experiments under the combined influence of greenhouse gases and surface aerosols, the fifth assessment report of the Intergovernmental Panel on Climate Change (IPCC, 2014) projected the global climate warming by 0.3 to 4.8°C during next 100 yr. Due to a lack of understanding of important climatic processes, the existence of many climatic and non-climatic systems, regional-scale variations and non-linearity, high degree of uncertainty among predictions of climate change impacts still predominated in several recent project scenarios. In another study, Rupa Kumar *et al.* (2002) used ECHAM4 and HadCM2 to project climatic scenarios over India for the periods 1980–2039 and 1920–1979. ECHAM4 predicted a 13% increase in monsoon rainfall, while HadCM2 predicted a 6% decrease. However, both models predicted a 1.0°C increase in mean annual temperature. At present, limited information is available on all-India or more local-scale seasonal composite scenarios, either derived directly from the GCMs outputs or using

some kind of downscaling method with finer resolution. On this backdrop, our effort was concentrated on the development of a Multi-Model Ensemble (MME) from the best performing models for constructing the future climate change scenarios over Western Ghats.

## Material and Methods

### Data requirement

IMD gridded temperature ( $1^\circ \times 1^\circ$ ) (Srivastava *et al.*, 2009) and rainfall ( $0.25^\circ \times 0.25^\circ$ ) (Pai *et al.*, 2014) data were used as observed data. The model simulations for both the present-day climate (historical experiments from 1969 to 2005 and 1901 to 2005 for temperature and rainfall, respectively under changing conditions consistent with observations) and future climate projections (RCP 2.6, RCP 4.5, RCP 6.0 and RCP 8.5 experiments from 2006 to 2100) are obtained from the CMIP5 data website (<http://pcmdi9.llnl.gov>). In this study, we selected models from the first ensemble member (r1i1p1) of each model. The details of the CMIP5 models used in the current study can be found elsewhere (Akhter *et al.*, 2017). Total 45 models were available for r1i1p1 ensemble of historical simulations. The number of models available for RCP 2.6, 4.5, 6.0 and 8.5 with ensemble r1i1p1 is 27, 43, 21 and 41, respectively. IMD gridded and GCM outputs are interpolated to the same resolution ( $0.25^\circ \times 0.25^\circ$ ) using bilinear interpolation technique. The monthly data over December–February, March–May, June–September and October–November representing winter, pre-monsoon, monsoon, post-monsoon seasons were averaged for temperature while sum was taken for rainfall.

### Trend test

We adapted the rank-based nonparametric Mann-Kendall (Kendall, 1948; Mann, 1945) method for assessing the long-term monotonic trend in time series (Sah *et al.*, 2020). Sen’s nonparametric method (Sen, 1968) was used to estimate the magnitude of trends in the time series data (Singh *et al.*, 2020).

### Model evaluation

For generation of future climate projections, first

step is the selection of the best performing models. We have used three approaches for evaluation of the CMIP5 models viz. trend analysis, conventional statistics and Taylor plot. Conventional statistics include following indices:

$$d\text{-index} = 1.0 - \left( \frac{\sum_{i=1}^n (O_i - M_i)^2}{\sum_{i=1}^n (|M_i - \bar{O}| + |O_i - \bar{M}|)} \right)$$

$$nRMSE = \sqrt{\frac{1}{n} \sum_{i=1}^n (O_i - M_i)^2} \times \frac{100}{\bar{O}}$$

$$pbias = \frac{\sum_{i=1}^n (O_i - M_i) \times 100}{\sum_{i=1}^n O_i}$$

$$r = \frac{\frac{1}{n} \sum_{i=1}^n (M_i - \bar{M})(O_i - \bar{O})}{\sigma_M \sigma_O}$$

$M_i$ : model output;  $\bar{M}$  and  $\sigma_M$ : mean and standard deviation of model output, respectively;  $O_i$ : observations;  $\bar{O}$  and  $\sigma_O$ : mean and standard deviation of observations, respectively. The best performing models were selected and averaged to have multimodel ensemble (MME).

### Taylor plot

Taylor plot presents a concise statistical overview of how well patterns matched with each other in terms of correlation, root-mean-square (RMS) difference, and variance ratio. The correlation coefficient and RMS difference provide complementary statistical information quantifying the correspondence between two patterns, but the variances (or standard deviations) of the fields must also be provided for a more complete characterization of the fields. All of these statistics are useful for pattern comparison, and the Taylor plot allows you to display them all on a single, easily interpreted diagram.

### Results and Discussion

The Mann-Kendall analysis of both temperature and rainfall revealed that the temperature was projected to increase significantly but rainfall would remain almost constant over the years. The Sen's

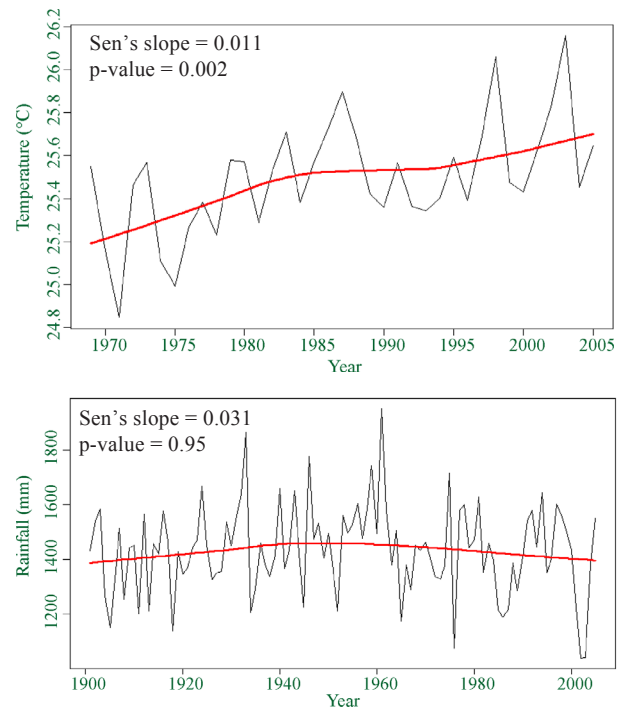


**Fig. 1.** Mann-Kendall trend test for temperature (upper panel) and rainfall (lower panel) over Western Ghats

slope for temperature was 0.011 ( $p = 0.002$ ) whereas it was 0.031 ( $p = 0.95$ ) for rainfall (Fig. 1).

The preliminary analysis for this study included computing the mean, standard deviation, and coefficient of seasonal and annual variation of temperature and precipitation time series for both for IMD datasets and CMIP-5 models. Table 1 and 2 presents these statistical parameters for the 37 (1969–2005) and 105 year (1901–2005) time period studied for temperature and rainfall variability, respectively. The mean annual temperature and rainfall varied between 23.11 and 29.22 °C and 484.24 and 2747.27 mm, respectively. The coefficient of variation indicating dispersion around the mean for temperature and rainfall was used to analyze the seasonal and annual spatial variability, both for IMD datasets and CMIP-5 models. This coefficient varied between 1.07 to 2.10% and 4.44 to 37.56% for temperature and rainfall, respectively.

For model evaluation, we have calculated linear trend of the CMIP-5 models for seasonal and annual time series. The models with similar trend as that of IMD gridded data were selected. Temperature trend

**Table 1.** Descriptive statistics for seasonal and annual temperature for the study region

	DJF				MAM				JIAS				ON				Annual			
	Mean	STDEV	CV	Mean	STDEV	CV														
IMD	23.74	0.44	1.87	28.03	0.36	1.28	25.35	0.33	1.31	24.62	0.38	1.53	25.50	0.26	1.02					
ACCESS1-0	25.58	0.42	1.66	29.50	0.43	1.45	27.45	0.47	1.71	26.93	0.70	2.60	27.41	0.33	1.20					
ACCESS1.3	27.07	0.50	1.84	31.34	0.52	1.67	29.28	0.59	2.01	29.17	0.62	2.13	29.22	0.41	1.40					
bc-c-esm1-1-m	26.58	0.36	1.34	30.13	0.57	1.90	25.67	0.56	2.19	26.30	0.65	2.46	27.12	0.33	1.22					
bc-c-esm1-1-m	26.23	0.46	1.74	30.41	0.34	1.12	26.39	0.40	1.52	26.91	0.46	1.71	27.44	0.29	1.07					
BNU-ESM	24.72	0.47	1.90	28.69	0.57	1.99	25.42	0.43	1.70	25.18	0.35	1.39	26.02	0.35	1.33					
CanESM2	25.19	0.50	1.98	29.09	0.79	2.70	26.42	0.63	2.40	25.14	0.55	2.18	26.57	0.50	1.89					
CCSM4	22.09	0.58	2.65	26.71	0.66	2.47	24.93	0.35	1.39	24.13	0.32	1.33	24.53	0.40	1.63					
CESMI-BGC	22.11	0.51	2.30	26.85	0.53	1.99	24.94	0.31	1.23	24.04	0.36	1.50	24.56	0.35	1.44					
CESMI-CAM5	21.57	0.59	2.73	26.01	0.69	2.67	24.13	0.38	1.59	23.41	0.31	1.32	23.84	0.42	1.78					
CESMI-WACCM	23.46	0.53	2.27	28.01	0.91	3.24	25.79	0.45	1.74	25.33	0.39	1.56	25.69	0.48	1.87					
CMCC-CM	23.73	0.60	2.54	29.07	0.39	1.33	25.65	0.48	1.88	24.67	0.46	1.85	25.86	0.37	1.44					
CMCC-CMS	23.71	0.70	2.96	29.64	0.63	2.13	25.92	0.76	2.93	24.80	0.63	2.54	26.11	0.55	2.10					
CNRM-CM5	22.91	0.54	2.35	27.49	0.46	1.69	25.19	0.35	1.39	23.09	0.47	2.04	24.85	0.33	1.32					
CSIRO-Mk3-6-0	26.79	0.48	1.80	30.17	0.40	1.33	29.19	0.47	1.60	28.53	0.64	2.23	28.72	0.33	1.15					
FIO-ESM	24.74	0.48	1.95	29.73	0.61	2.06	26.56	0.50	1.88	25.87	0.37	1.45	26.78	0.39	1.46					
GISS-E2-H	26.14	0.45	1.73	28.90	0.39	1.35	26.11	0.50	1.92	26.82	0.67	2.51	26.94	0.38	1.40					
GISS-E2-R	26.36	0.46	1.73	29.36	0.40	1.35	26.38	0.50	1.91	26.68	0.58	2.19	27.17	0.31	1.16					
GISS-E2-H-CG	26.69	0.41	1.53	29.20	0.38	1.31	26.49	0.47	1.79	27.14	0.63	2.32	27.33	0.34	1.23					
HadGEM2-AO	25.53	0.41	1.60	29.31	0.41	1.40	27.11	0.51	1.86	26.92	0.63	2.33	27.23	0.40	1.46					
HadGEM2-CC	28.50	0.42	1.48	25.96	0.40	1.56	25.27	0.49	1.94	26.48	0.36	1.35	26.45	0.31	1.19					
HadGEM2-ES	29.00	0.38	1.32	26.35	0.51	1.94	25.66	0.57	2.24	27.01	0.39	1.44	26.91	0.42	1.56					
inmcm4	20.33	0.64	3.14	24.42	0.47	1.92	24.37	0.38	1.56	22.81	0.57	2.50	23.11	0.28	1.19					
IPSL-CM5A-MR	23.59	0.40	1.69	27.55	0.66	2.38	26.42	0.53	2.00	24.97	0.37	1.50	25.75	0.43	1.65					
IPSL-CM5B-LR	24.06	0.38	1.57	27.58	0.38	1.38	27.55	0.54	1.96	25.48	0.50	1.97	26.34	0.35	1.33					
MIROC-ESM-CHEM	23.23	0.37	1.60	28.38	0.56	1.99	24.86	0.25	1.01	24.49	0.29	1.20	25.27	0.28	1.12					
MIROC-ESM	23.19	0.39	1.68	28.23	0.48	1.70	24.79	0.33	1.33	24.43	0.32	1.33	25.19	0.30	1.20					
MIROC5	24.55	0.44	1.81	28.37	0.60	2.12	26.22	0.41	1.56	25.45	0.58	2.26	26.21	0.38	1.44					
MPI-ESM-LR	23.14	0.73	3.14	28.83	0.59	2.04	25.34	0.52	2.06	24.58	0.76	3.09	25.53	0.50	1.96					
MPI-ESM-MR	22.91	0.46	1.99	28.84	0.49	1.69	25.43	0.49	1.92	24.27	0.54	2.21	25.46	0.38	1.50					
MPI-ESM-P	23.30	0.64	2.76	28.91	0.46	1.59	25.37	0.42	1.66	24.59	0.59	2.39	25.61	0.37	1.43					
MRI-CGCM3	24.09	0.60	2.50	29.09	0.44	1.52	25.94	0.61	2.34	24.97	0.79	3.16	26.10	0.41	1.58					
MRI-ESM1	24.14	0.64	2.64	29.29	0.47	1.60	26.08	0.67	2.58	25.21	0.84	3.31	26.25	0.41	1.55					
NorESM1-M	22.55	0.46	2.06	27.79	0.54	1.93	25.25	0.43	1.72	24.67	0.46	1.87	25.11	0.40	1.59					
NorESM1-ME	22.49	0.59	2.63	27.57	0.64	2.33	25.14	0.38	1.52	24.55	0.39	1.58	24.99	0.44	1.75					

Table 2. Descriptive statistics for seasonal and annual Rainfall for the study region

	DJF				MAM				JJAS				ON				Annual			
	Mean	STDEV	CV	Mean	STDEV	CV	Mean	STDEV	CV	Mean	STDEV	CV	Mean	STDEV	CV	Mean	STDEV	CV		
IMD	40.97	26.74	65.27	164.71	52.43	31.83	976.43	140.40	14.38	252.03	71.23	28.26	1434.72	162.83	11.35					
ACCESS1-0	40.77	25.07	61.49	44.43	22.02	49.56	507.64	116.97	23.04	73.45	41.28	56.20	666.29	130.41	19.57					
ACCESS1.3	98.34	52.24	53.12	42.93	23.57	54.91	365.68	108.40	29.64	110.68	62.07	56.08	617.64	147.42	23.87					
bcc-csm1-1	56.56	37.24	65.85	98.49	70.25	71.32	1456.90	291.20	19.99	288.92	120.09	41.57	1900.88	315.75	16.61					
bcc-csm1-1-m	71.21	26.67	37.45	203.45	104.84	51.53	1456.41	272.52	18.71	256.47	89.00	34.70	1987.54	324.62	16.33					
BNU-ESM	93.21	52.43	56.25	239.24	86.77	36.27	1285.13	176.07	13.70	320.97	100.94	31.45	1938.55	284.53	14.68					
CanESM2	118.73	23.25	19.58	106.69	21.38	20.04	713.27	57.47	8.06	247.79	30.23	12.20	1186.48	87.95	7.41					
CCSM4	143.69	27.28	18.99	149.25	26.70	17.89	1221.89	48.27	3.95	312.55	33.23	10.63	1827.38	88.65	4.85					
CESM1-BGC	134.54	65.09	48.38	132.05	57.67	43.67	1230.36	116.85	9.50	295.52	85.76	29.02	1792.48	204.33	11.40					
CESM1-CAM5	154.03	47.10	30.58	173.50	39.31	22.66	1220.11	69.99	5.74	348.01	47.78	13.73	1895.65	135.02	7.12					
CMCC-CM	30.16	26.53	87.99	23.49	18.45	78.55	691.90	125.80	18.18	178.45	59.56	33.37	923.99	136.60	14.78					
CMCC-CMS	48.82	34.77	71.23	28.89	25.77	89.20	883.33	175.89	19.91	214.49	80.63	37.59	1175.53	168.11	14.30					
CNRM-CM5	66.15	36.88	55.75	154.52	39.01	25.24	618.18	80.02	12.94	211.42	63.25	29.92	1050.26	126.09	12.01					
CSIRO-Mk3-6-0	59.08	15.26	25.83	38.88	7.19	18.49	241.52	25.70	10.64	144.76	30.60	21.14	484.24	48.61	10.04					
EC-EARTH	83.14	20.66	24.84	198.87	31.94	16.06	1034.63	56.46	5.46	229.85	35.28	15.35	1546.49	68.67	4.44					
FGOALS_g2	91.83	56.89	61.96	140.04	45.93	32.79	2286.64	303.74	13.28	228.76	90.03	39.36	2747.27	301.35	10.97					
FIO-ESM	101.83	31.88	31.31	99.64	30.82	30.93	1180.15	121.68	10.31	283.81	51.42	18.12	1665.44	154.92	9.30					
GFDL-CM3	56.91	33.64	59.12	154.09	29.23	18.97	742.45	86.61	11.67	276.60	69.95	25.29	1230.05	139.64	11.35					
GFDL-ESM2G	48.45	32.66	67.42	162.67	47.96	29.48	868.22	105.55	12.16	279.68	79.05	28.26	1359.02	161.28	11.87					
GFDL-ESM2M	78.68	55.23	70.20	185.76	75.91	40.87	983.04	146.27	14.88	293.56	108.88	37.09	1541.04	243.88	15.83					
GISS-E2-H	53.39	12.10	22.66	90.03	12.67	14.07	1115.86	112.55	10.09	136.00	25.89	19.04	1395.27	124.27	8.91					
GISS-E2-H	55.04	11.56	21.00	89.19	11.73	13.15	1123.66	112.98	10.06	137.18	25.74	18.77	1405.07	128.31	9.13					
GISS-E2-H	52.84	10.85	20.53	90.59	11.22	12.39	1267.03	84.58	6.68	124.69	18.98	15.22	1535.16	88.05	5.74					
GISS-E2-H-CC	54.70	24.39	44.58	84.34	24.01	28.47	1030.43	202.66	19.67	131.31	57.25	43.60	1300.78	203.25	15.63					
GISS-E2-R	64.05	12.75	19.91	85.40	12.28	14.38	1049.24	83.92	8.00	157.07	23.05	14.67	1355.76	97.86	7.22					
GISS-E2-R	62.03	12.48	20.12	87.42	12.17	13.92	1003.55	85.80	8.55	155.14	27.82	17.94	1308.14	105.47	8.06					
GISS-E2-R	60.13	12.19	20.27	84.42	9.79	11.60	1072.86	77.68	7.24	144.06	22.10	15.34	1361.48	87.93	6.46					
GISS-E2-R-CC	65.01	29.41	45.25	86.66	28.30	32.65	1021.47	163.01	15.96	166.81	69.81	41.85	1339.95	188.45	14.06					
HadGEM2-AO	28.92	17.77	61.46	30.60	15.50	50.67	473.72	118.79	25.08	62.84	32.99	52.51	596.07	130.32	21.86					
HadGEM2-CC	33.25	17.45	52.47	24.90	14.00	56.24	410.12	128.37	31.30	74.99	41.54	55.40	543.26	137.67	25.34					
HadGEM2-ES	32.89	10.53	32.00	26.29	7.25	27.56	416.74	57.65	13.83	71.28	19.72	27.67	547.20	62.84	11.48					
inmcm4	205.43	83.76	40.77	197.30	86.97	44.08	1055.26	125.33	11.88	521.94	95.19	18.24	1979.94	251.63	12.71					

IPSL-CM5A-LR	49.18	15.88	32.30	102.23	20.38	19.94	430.18	64.05	14.89	232.51	28.84	12.41	814.09	88.98	10.93
IPSL-CM5A-MR	42.35	29.40	69.42	119.18	50.26	42.17	611.68	150.42	24.59	242.50	61.43	25.33	1015.71	197.11	19.41
IPSL-CM5B-LR	22.64	21.18	93.57	13.28	5.94	44.73	412.35	204.72	49.65	116.14	81.52	70.19	564.42	211.99	37.56
MIROC5	100.78	29.60	29.37	336.25	45.38	13.50	866.60	70.23	8.10	212.94	44.14	20.73	1516.57	96.67	6.37
MIROC-ESM	89.26	38.22	42.82	214.94	70.54	32.82	1482.29	88.03	5.94	359.04	46.06	12.83	2145.54	118.43	5.52
MIROC-ESM-CHEM	87.36	35.76	40.93	211.57	58.25	27.53	1469.53	86.73	5.90	360.99	42.49	11.77	2129.45	117.77	5.53
MPI-ESM-LR	28.92	14.51	50.16	82.72	37.90	45.82	721.45	57.35	7.95	188.75	43.47	23.03	1021.84	92.17	9.02
MPI-ESM-MR	23.44	12.05	51.39	78.80	30.12	38.22	860.64	62.77	7.29	207.11	45.30	21.87	1169.98	84.28	7.20
MRI-CGCM3	24.81	18.65	75.15	25.57	15.94	62.35	414.58	135.82	32.76	161.28	84.93	52.66	626.24	162.39	25.93
NorESM1-M	92.89	48.04	51.72	58.98	24.33	41.25	1039.60	165.14	15.89	260.49	85.27	32.73	1451.95	228.91	15.77
NorESM1-ME	101.03	55.26	54.70	64.99	30.26	46.56	1039.35	137.82	13.26	296.34	98.07	33.09	1501.71	220.44	14.68

of IMD gridded data for both seasonal and annual cycle was positive that confirmed a warming trend over the study period (1969-2005). Most of the models showed positive trend for annual cycle except MIROC-ESM-CHEM (Table 3). Rainfall Trend of IMD gridded data was negative for both annual and seasonal cycle except for monsoon season. The CMIP-5 models revealed variable trends for rainfall pattern (Table 4). For annual cycle, ACCESS1-0, bcc-csm1-1, bcc-csm1-1-m, CESM1-BGC, EC-EARTH, FGOALS-g2, GFDL-ESM2M, GISS-E2-R, HadGEM2-ES, IPSL-CM5A-LR, IPSL-CM5A-MR, MIROC5, MIROC-ESM, MPI-ESM-LR, MRI-CGCM3 and NorESM1-M models showed positive trend.

Conventional statistics were used to select the best performing models. For temperature, the models which were having d-index >0.95, nRMSE <50, pbias between -10 to 10 and correlation >0.95 were selected. The selected models based on the criteria were BNU-ESM, CESM1-WACCM, MIROC-ESM-CHEM, MIROC-ESM, MPI-ESM-LR, MPI-ESM-MR, MPI-ESM-P, NorESM1-M, and NorESM1-ME (Table 5). For rainfall dynamics, the selection criteria were slightly loosened likely d-index >0.90, nRMSE <50, pbias between -20 to 20 and correlation >0.85 as the average model performances were little bit poor. On the basis of these criteria, the selected rainfall models were CMCC-CMS, EC-EARTH, GFDL-CM3, GFDL-ESM2G, GFDL-ESM2M, MIROC5, MPI-ESM-MR and NorESM1-M (Table 6).

Performance of the best GCMs was assessed using Taylor Diagram with reference to IMD gridded data (Fig. 2). The results indicated that all the selected models were efficient to simulate IMD gridded observed temperature and rainfall with adequate accuracy. Seasonal plotting of past observed and multi-model ensemble data showed a good agreement for temperature (Fig. 3), but multi-model ensemble for rainfall failed to simulate observed rainfall for July and September. We developed a Multi Model Ensemble (MME9, MME8 for temperature and rainfall, respectively) from the best performing models for both past and future time period (1969-2100 and 1901-2100 for temperature and rainfall, respectively) (Fig. 4). MME9 indicated

**Table 3.** Linear trend of IMD gridded and CMIP-5 model data for temperature over Western Ghats

Trend ( $^{\circ}\text{C}/37 \text{ yr}$ )	Annual	DJF	MAM	JJAS	ON
IMD	0.48	0.73	0.27	0.51	0.42
ACCESS1-0	0.47	0.54	0.64	0.32	0.40
ACCESS1.3	0.35	0.34	0.63	0.28	0.08
bcc-csm1-1-m	0.36	0.14	0.46	0.70	-0.11
bcc-csm1-1	0.71	0.81	0.70	0.78	0.41
BNU-ESM	0.64	0.12	1.00	0.75	0.67
CanESM2	0.86	0.98	0.78	0.90	0.76
CCSM4	0.61	0.52	0.68	0.69	0.51
CESM1-BGC	0.43	0.30	0.46	0.41	0.59
CESM1-CAM5	0.36	0.53	0.25	0.33	0.35
CESM1-WACCM	0.35	0.06	0.21	0.62	0.44
CMCC-CM	0.15	-0.13	0.77	0.03	-0.10
CMCC-CMS	0.66	0.60	1.11	0.43	0.56
CNRM-CM5	0.71	0.80	0.69	0.69	0.65
CSIRO-Mk3-6-0	0.59	0.56	0.44	0.69	0.69
FIO-ESM	0.62	0.78	0.81	0.38	0.56
GISS-E2-H	0.79	0.73	0.74	0.88	0.76
GISS-E2-R	0.29	0.46	0.42	0.14	0.15
GISS-E2-H-CC	0.43	0.72	0.42	0.41	0.05
HadGEM2-AO	0.83	0.78	0.74	1.01	0.68
HadGEM2-CC	0.48	0.83	0.45	0.32	0.38
HadGEM2-ES	0.44	0.36	0.45	0.23	0.29
inmcm4	0.45	0.32	0.79	0.42	0.22
IPSL-CM5A-MR	1.00	0.94	1.01	1.11	0.83
IPSL-CM5B-LR	0.70	0.60	0.44	1.10	0.41
MIROC-ESM-CHEM	-0.14	-0.25	-0.56	0.17	0.06
MIROC-ESM	0.14	0.05	-0.13	0.48	0.01
MIROC5	0.70	0.49	0.90	0.98	0.15
MPI-ESM-LR	0.71	0.30	0.86	0.86	0.82
MPI-ESM-MR	0.80	0.80	0.86	0.73	0.86
MPI-ESM-P	0.60	0.54	0.57	0.63	0.70
MRI-CGCM3	0.33	0.26	0.32	0.33	0.46
MRI-ESM1	0.18	-0.19	0.18	0.35	0.37
NorESM1-M	0.75	0.73	0.78	0.72	0.80
NorESM1-ME	0.75	0.84	0.59	0.75	0.83

**Table 4.** Linear trend of IMD gridded and CMIP-5 model data for rainfall over Western Ghats

Trend (mm/105 yr)	DJF	MAM	JJAS	ON	Annual
IMD	-17.74	-16.64	30.32	-12.53	-15.92
ACCESS1-0	-9.30	-2.27	53.66	5.45	47.55
ACCESS1.3	-7.87	-4.50	-46.57	-25.44	-84.38
bcc-csm1-1	10.80	1.34	6.93	50.89	69.96
bcc-csm1-1-m	15.33	71.05	145.30	47.56	279.24
BNU-ESM	-14.92	-66.55	54.70	25.58	-1.19
CanESM2	-36.52	7.40	4.54	-13.75	-38.33
CCSM4	-1.08	-21.12	27.41	15.95	21.16
CESM1-BGC	-8.88	-24.14	-34.50	24.60	-42.91
CESM1-CAM5	-7.68	15.83	-77.71	-6.96	-76.51
CMCC-CM	-4.44	9.85	80.09	-45.62	39.89
CMCC-CMS	4.86	3.00	-0.29	-35.68	-28.11
CNRM-CM5	-23.20	-13.02	5.24	-6.08	-37.06
CSIRO-Mk3-6-0	-3.45	-0.06	-18.28	0.44	-21.35
EC-EARTH	-8.98	10.90	74.84	12.15	88.91
FGOALS_g2	-0.68	9.71	132.26	25.54	166.83
FIO-ESM	-5.38	-6.71	22.43	-39.79	-29.45
GFDL-CM3	-1.08	-10.27	11.28	-22.30	-22.36
GFDL-ESM2G	6.00	-15.73	-5.61	12.18	-3.15
GFDL-ESM2M	-7.53	-16.37	25.47	19.64	21.22
GISS-E2-H	-12.31	-1.32	-143.88	-4.42	-161.92
GISS-E2-H	-11.84	5.76	-176.08	-25.28	-207.44
GISS-E2-H	1.21	7.58	-65.96	18.48	-38.70
GISS-E2-H-CC	-11.66	2.10	-88.38	15.53	-82.42
GISS-E2-R	-14.49	-5.58	-112.48	-18.82	-151.37
GISS-E2-R	-10.44	-4.18	-109.71	-20.73	-145.06
GISS-E2-R	-7.68	7.38	54.99	4.64	59.33
GISS-E2-R-CC	-26.99	-22.22	-28.29	-26.55	-104.05
HadGEM2-AO	-7.32	1.03	-75.28	-2.04	-83.61
HadGEM2-CC	-4.53	-3.10	-5.66	26.65	13.37
HadGEM2-ES	-3.61	1.58	-20.92	2.28	-20.68
inmcm4	-21.70	-20.59	-8.27	30.42	-20.14
IPSL-CM5A-LR	3.62	-5.35	22.87	29.95	51.10
IPSL-CM5A-MR	5.44	8.21	3.46	-1.17	15.94
IPSL-CM5B-LR	-8.52	-0.28	-137.81	-5.77	-152.37
MIROC5	-34.51	-20.07	19.57	55.44	20.43
MIROC-ESM	6.19	-6.39	61.59	-28.99	32.41
MIROC-ESM-CHEM	-0.22	-34.70	-42.79	-2.59	-80.30
MPI-ESM-LR	4.21	15.74	-20.60	38.40	37.76
MPI-ESM-MR	-6.31	-1.53	-18.86	-2.39	-29.09
MRI-CGCM3	-16.09	-1.93	89.37	-41.29	30.06
NorESM1-M	-8.51	0.93	-3.17	13.50	2.75
NorESM1-ME	9.99	-4.90	-6.24	-8.20	-9.36

**Table 5.** Performance of the CMIP-5 models for prediction of temperature over Western Ghats

	d-index	nRMSE	pbias	Correlation
ACCESS1-0	0.76	110.6	7.5	0.96
ACCESS1.3	0.54	212.6	14.6	0.92
bcc-csm1-1-m	0.76	110.6	6.4	0.82
bcc-csm1-1	0.76	117.3	7.6	0.92
BNU-ESM	0.96	37	2.1	0.97
CanESM2	0.88	70	4.2	0.93
CCSM4	0.88	68.1	-3.8	0.91
CESM1-BGC	0.9	63.6	-3.7	0.94
CESM1-CAM5	0.79	97.5	-6.5	0.95
CESM1-WACCM	0.98	28.7	0.7	0.96
CMCC-CM	0.95	49.8	1.4	0.96
CMCC-CMS	0.93	60.6	2.4	0.98
CNRM-CM5	0.94	51.7	-2.5	0.95
CSIRO-Mk3-6-0	0.54	186.3	12.7	0.9
FIO-ESM	0.88	77.5	5	0.98
GISS-E2-H	0.77	93.7	5.6	0.87
GISS-E2-R	0.76	103.1	6.6	0.9
GISS-E2-H-CC	0.7	114.7	7.2	0.85
HadGEM2-AO	0.78	100.3	6.8	0.97
inmcm4	0.62	154.9	-9.3	0.72
IPSL-CM5A-MR	0.95	43	1	0.91
IPSL-CM5B-LR	0.82	81.6	3.3	0.76
MIROC-ESM-CHEM	0.98	30.2	-0.9	0.98
MIROC-ESM	0.98	30.2	-1.2	0.98
MIROC5	0.94	44.6	2.8	0.99
MPI-ESM-LR	0.98	31.6	0.2	0.99
MPI-ESM-MR	0.97	40.6	-0.1	0.99
MPI-ESM-P	0.98	31.8	0.4	0.99
MRI-CGCM3	0.95	50.3	2.4	0.97
MRI-ESM1	0.93	57.7	3	0.97
NorESM1-M	0.96	40.7	-1.5	0.96
NorESM1-ME	0.95	44.6	-2	0.95

**Table 6.** Performance of the CMIP-5 models for prediction of rainfall over Western Ghats

	d-index	nRMSE	pbias	Correlation
ACCESS1-0	0.78	80.1	-53.6	0.86
ACCESS1-3	0.61	99.5	-57	0.6
bcc-csm1-1	0.89	84.6	32.5	0.93
bcc-csm1-1-m	0.91	70.2	38.5	0.96
BNU-ESM	0.95	51.2	35.1	0.98
CanESM2	0.84	61.9	-17.3	0.8
CCSM4	0.95	48.3	27.4	0.95
CESM1-BGC	0.95	46.2	24.9	0.95
CESM1-CAM5	0.94	51.4	32.1	0.94
CMCC-CM	0.88	59.1	-35.6	0.89
CMCC-CMS	0.93	47.6	-18.1	0.9
CNRM-CM5	0.84	60	-26.8	0.92
CSIRO-Mk3-6-0	0.56	107.1	-66.2	0.75
EC-EARTH	0.97	31.8	7.8	0.95
FGOALS_g2	0.7	190.3	91.5	0.9
FIO-ESM	0.94	50.9	16.1	0.91
NOAA	0.91	48.2	-14.3	0.9
NOAA.1	0.95	37.2	-5.3	0.93
NOAA.2	0.97	31.6	7.4	0.95
GISS-E2-H	0.9	65.2	-2.7	0.85
GISS-E2-H.1	0.89	72.1	-2.1	0.82
GISS-E2-H.2	0.88	77.9	7	0.85
GISS-E2-H-CC	0.89	68.3	-9.3	0.81
GISS-E2-R	0.88	69.4	-5.5	0.8
GISS-E2-R.1	0.88	69.9	-8.8	0.78
GISS-E2-R.2	0.88	72.4	-5.1	0.79
GISS-E2-R-CC	0.89	66.6	-6.6	0.81
HadGEM2-AO	0.75	84.7	-58.5	0.87
HadGEM2-CC	0.71	90.5	-62.1	0.87
HadGEM2-ES	0.71	90.2	-61.9	0.86
inmcm4	0.85	74.6	38	0.79
IPSL-CM5A-LR	0.68	87	-43.3	0.66
IPSL-CM5A-MR	0.82	68.9	-29.2	0.78
IPSL-CM5B-LR	0.65	107.5	-60.7	0.5
MIROC5	0.92	45.5	5.7	0.89
MIROC-ESM	0.9	76	49.5	0.96
MIROC-ESM-CHEM	0.9	74	48.4	0.96
MPI-ESM-LR	0.93	45	-28.8	0.97
MPI-ESM-MR	0.96	34	-18.5	0.96
MRI-CGCM3	0.72	88.7	-56.4	0.78
NorESM1-M	0.95	44.1	1.2	0.91
NorESM1-ME	0.93	50.9	4.7	0.88

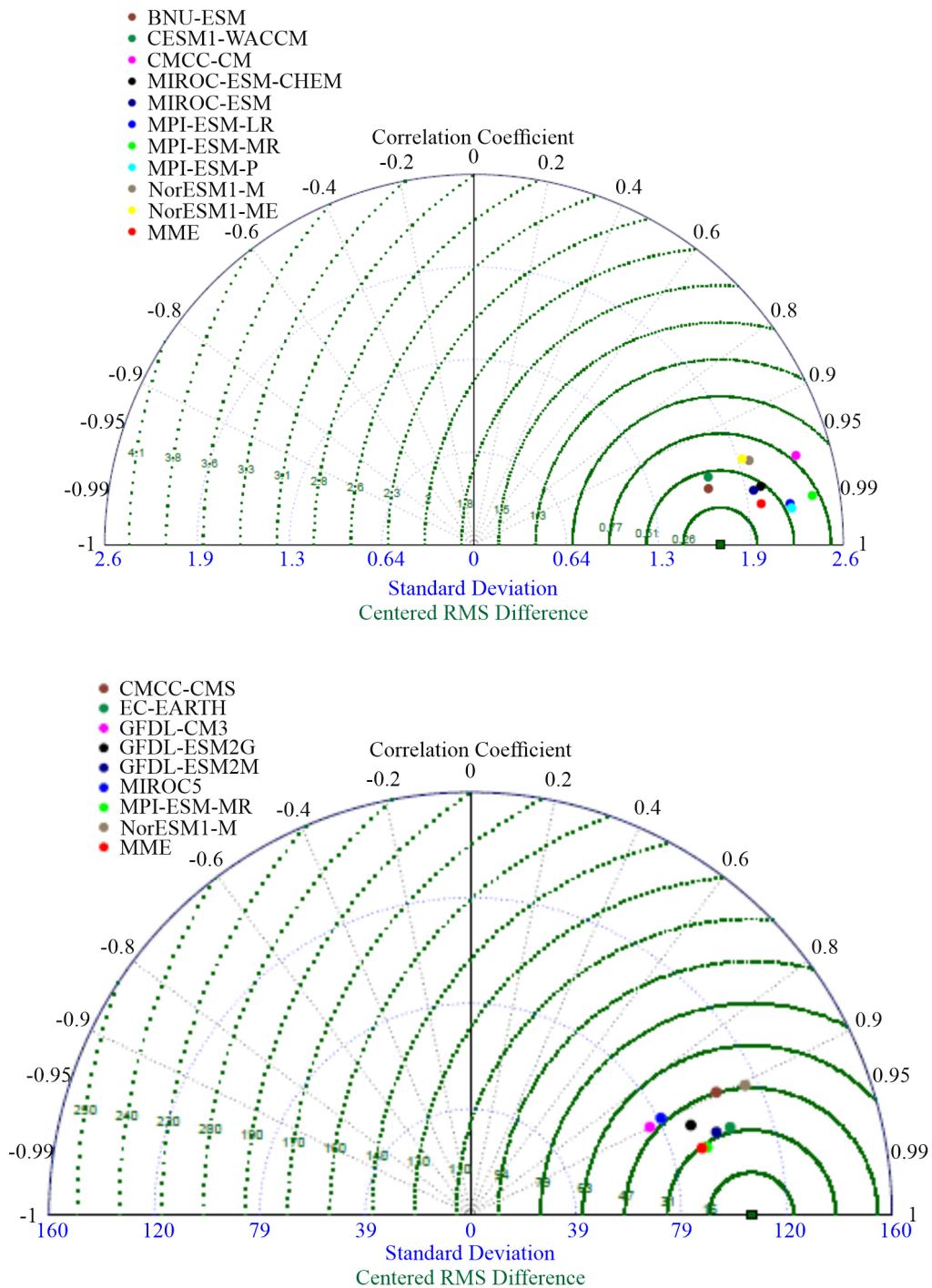


**Fig. 2.** Taylor plot of temperature (upper panel) and rainfall (lower panel) over Western Ghats

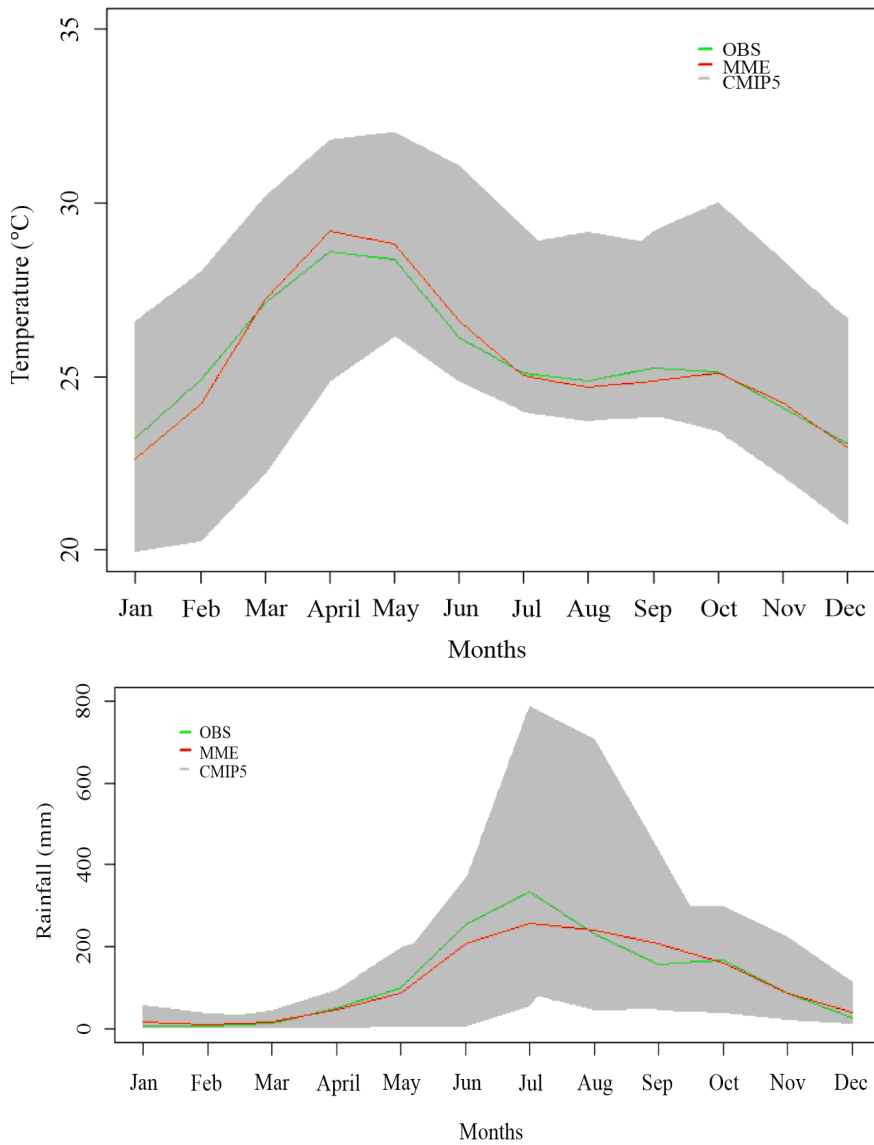


**Fig. 3.** Mean seasonal cycle of temperature (upper panel) and rainfall (lower panel) over Western Ghats

**Table 7.** Percentage change in temperature and rainfall for 2006-2100 over the study area

	RCP2.6	RCP4.5	RCP6.0	RCP8.5
Base period	4.19 (1.08 °C)	6.36 (1.62 °C)	4.72 (1.20 °C)	9.31 (2.37 °C)
Base period	-0.78 (-11.12 mm)	-2.35 (-33.16 mm)	4.99 (71.49 mm)	0.01 (0.17 mm)

that temperature was projected to increase around 4.19-9.31% for different RCPs during 2006-2100 with reference to the base period of 1970-2000 (RCP2.6 = 4.19, RCP4.5 = 6.36, RCP6.0 = 4.72 and

RCP8.5 = 9.31%). The multi-model ensemble for rainfall (MME8) indicated a very marginal increase in rainfall in RCP2.6 and RCP6.0, but it might decrease according to RCP4.5 and RCP8.5 (-0.78, -

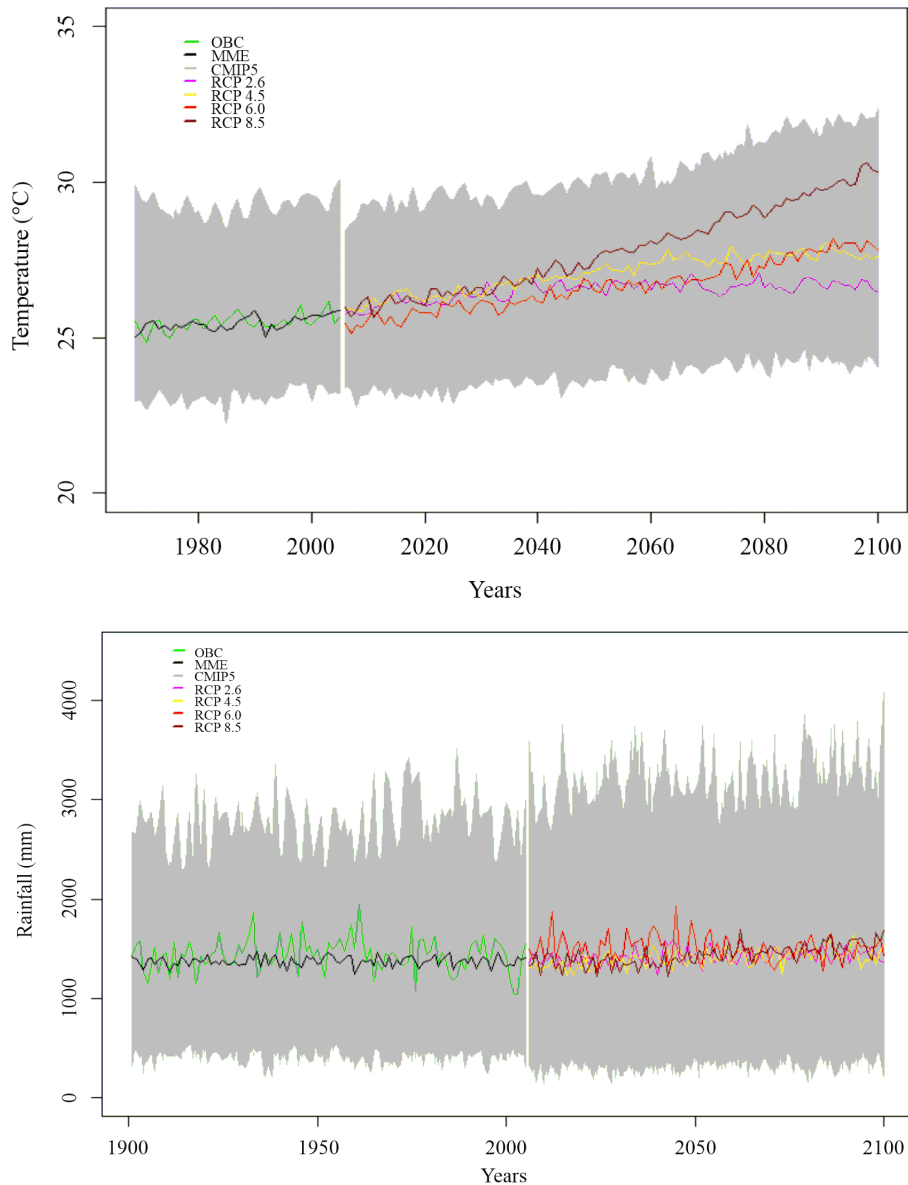


**Fig. 4.** Past and future temperature time series for temperature (upper panel) and rainfall (lower panel) over Western Ghats

2.35, 4.99 and 0.01% for RCP2.6, RCP4.5, RCP6.0 and RCP8.5, respectively) (Table 7).

## Conclusions

The GCM models were able to simulate the temperature but the performance of the models to simulate rainfall was found to be poor. In general, future temperature may increase which may increase the plant water requirement through increasing evapotranspiration. But rainfall may not increase

significantly. So, rainfed agriculture in the study region may face acute water crises in future.

## References

- Akhter, J., Das, L. and Deb, A. 2017. CMIP5 ensemble-based spatial rainfall projection over homogeneous zones of India. *Climate Dynamics* **49**: 1885–1916. <https://doi.org/10.1007/s00382-016-3409-8>
- Benestad, R.E. 2002. Empirically Downscaled Multimodel Ensemble Temperature and

- Precipitation Scenarios for Norway. *Journal of Climate* **15**: 3008–3027.
- Chaturvedi, R.K., Joshi, J., Jayaraman, M., Bala, G. and Ravindranath, N.H. 2012. Multi-model climate change projections for India under representative concentration pathways. *Current Science* **103**: 791–802.
- Daron, J., Macadam, I., Kanamaru, H., Cinco, T., Katzfey, J., Scannell, C., Jones, R., Villafuerte, M., Cruz, F., Narisma, G., Delfino, R.J., Lasco, R., Manalo, J., Ares, E., Solis, A.L., de Guzman, R., Basconcillo, J. and Tangang, F. 2018. Providing future climate projections using multiple models and methods: insights from the Philippines. *Climatic Change* **148**: 187–203. <https://doi.org/10.1007/s10584-018-2183-5>
- Das, L. and Akhter, J. 2019. How well are the downscaled CMIP5 models able to reproduce the monsoon precipitation over seven homogeneous zones of India? *International Journal of Climatology* **39**: 3323–3333. <https://doi.org/10.1002/joc.6022>
- Das, L., Akhter, J., Dutta, M. and Meher, J.K. 2015. Ensemble-based CMIP5 simulations of monsoon rainfall and temperature changes over South Asia. pp. 41–60. <https://doi.org/10.13140/RG.2.1.1861.4160>
- Das, L., Meher, J.K., Akhter, J., Benestad, R.E. and Mezghani, A. 2014. Assessing the performance of CMIP5 GCMs in simulating the observed annual and seasonal rainfall over the Western Himalayan Region of India Assessing the performance of CMIP5 GCMs in simulating the observed annual and seasonal rainfall over the Western Him. *Journal of Agrometeorology* **16**: 139–142.
- Das, L., Nagaraj, K. and Nanda, M.K., 2012. Construction of all-India seasonal future climate scenarios using GCMs output/ : Effect of greenhouse gas and sulphate aerosols. *Journal of Agrometeorology* **14**: 299–311.
- Gharbia, S.S., Gill, L., Johnston, P. and Pilla, F. 2016. Multi-GCM ensembles performance for climate projection on a GIS platform. *Model. Earth Syst. Environ.* **2**: 102. <https://doi.org/10.1007/s40808-016-0154-2>
- Grotch, S.L. and MacCracken, M.C. 1991. The Use of General Circulation Models to Predict Regional Climatic Change. *Journal of Climate* **4**: 286–303.
- Hirakuchi, H. and Giorgi, F. 1995. Multiyear present-day and  $2 \times \text{CO}_2$  simulations of monsoon climate over eastern Asia and Japan with a regional climate model nested in a general circulation model. *J. Geophys. Res.*, **100**: 21105–21125. <https://doi.org/10.1029/95JD01885>
- Huth, R. and Kysely, J. 2000. Constructing site-specific climate change scenarios on a monthly scale using statistical downscaling. *Theor. Appl. Climatol.* **66**: 13–27. <https://doi.org/10.1007/s007040070030>
- Kaur, J., Kaur, P. and Kaur, S. 2020. Climate change predictions by ensemble model in different agroclimatic zones of Punjab, India. *Journal of Agricultural Physics* **20**: 231–242.
- Kendall, M.G. 1948. Rank correlation methods. Griffin.
- Kidson, J.W. and Thompson, C.S. 1998. A comparison of statistical and model-based downscaling techniques for estimating local climate variations. *Journal of Climate* **11**: 735–753.
- Kripalani, R.H., Kulkarni, A., Sabade, S.S. and Khandekar, M.L. 2003. Indian monsoon variability in a global warming scenario. *Natural Hazards* **29**: 189–206. <https://doi.org/10.1023/A:1023695326825>
- Lal, M., Cubasch, U. and Santer, B.D. 1994. Effect of global warming on Indian monsoon simulated with a coupled ocean-atmosphere general circulation model. *Current Science* **66**: 430–438.
- Mann, H.B. 1945. Nonparametric Tests Against Trend. *Econometrica* **13**: 245–259.
- Ngai, S.T., Tangang, F. and Juneng, L. 2017. Bias correction of global and regional simulated daily precipitation and surface mean temperature over Southeast Asia using quantile mapping method. *Global and Planetary Change* **149**: 79–90.
- Pai, D.S., Sridhar, L., Rajeevan, M., Sreejith, O.P., Satbhai, N.S. and Mukhopadhyay, B. 2014. Development of a new high spatial resolution ( $0.25 \times 0.25$ ) long period (1901–2010) daily gridded rainfall data set over India and its comparison with existing data sets over the region. *Mausam* **65**: 1–18.
- Rupa Kumar, K., Krishna Kumar, K., Ashrit, R.G., Patwardhan, S.K. and Pant, G.B. 2002. Climate change in India: Observations and model projections. *Clim. Chang. India Issues, Concerns Oppor.* Tata McGraw-Hill Publ. Co. Limited, New Delhi.
- Sah, S., Singh, R.N., Chaturvedi, G. and Das, B. 2021. Trends, variability, and teleconnections of long-

- term rainfall in the Terai region of India. *Theoretical and Applied Climatology* **143**: 291–307 <https://doi.org/10.1007/s00704-020-03421-y>
- Sen, P.K. 1968. Estimates of the Regression Coefficient Based on Kendall's Tau. *Journal of the American Statistical Association* **63**: 1379–1389. <https://doi.org/10.2307/2285891>
- Singh, R.N., Sah, S., Das, B., Potekar, S., Chaudhary, A. and Pathak, H. 2021. Innovative trend analysis of spatio-temporal variations of rainfall in India during 1901–2019. *Theoretical and Applied Climatology* **145**: 821–838. <https://doi.org/10.1007/s00704-021-03657-2>
- Singh, R.N., Sah, S., Das, B., Vishnoi, L. and Pathak, H. 2021. Spatio-temporal trends and variability of rainfall in Maharashtra, India: Analysis of 118 years. *Theoretical and Applied Climatology* **143**: 883–900. <https://doi.org/10.1007/s00704-020-03452-5>
- Srivastava, A.K., Rajeevan, M. and Kshirsagar, S.R. 2009. Development of a high resolution daily gridded temperature data set (1969–2005) for the Indian region. *Atmospheric Science Letters* **10**: 249–254. <https://doi.org/10.1002/asl.232>

---

Received: July 25, 2021; Accepted: October 22, 2021